An inter-laboratory study on the stability of all-printable HTM-free perovskite solar cells

F. De Rossi[a, b]*, J. Barbe[a], D. Tanenbaum[c], L. Cinà[b,d], V. Stoichkov[e], Z. Wei[a], W.C. Tsoi[a], J. Kettle[e], A. Sadula[f], B. Azzopardi[f], Haibing Xie[c], M. Lira-Cantú[c], E. A. Katz[b,g], T.M. Watson[a], and F. Brunetti[b]

[a] *SPECIFIC - Swansea University, Bay Campus, Fabian Way, Swansea, SA1 8EN (UK)*

[b] *University of Rome Tor Vergata*

[c] Catalan Institute of Nanoscience and Nanotechnology (ICN2), CSIC and the Barcelona Institute of Science and Technology (BIST). Building ICN2, Campus UAB E-08193, Bellaterra, Barcelona, Spain.

[d] *Cicci Research*

[e] *School of Computer Science and Electronic Engineering, Bangor University, Dean St, Bangor, Gwynedd, LL57 1UT, Wales*

[f] *MCAST Malta*

[g] *Department of Solar Energy and Environmental Physics, Swiss Institute for Dryland Environmental and Energy Research, Jacob Blaustein Institutes for Desert Research, Ben-Gurion University of the Negev, Midreshet Ben-Gurion 8499000, Israel*

please add your institution's address

Abstract

Halide perovskite solar cells (PSCs) have revolutionized the photovoltaic arena providing power conversion efficiencies currently above 25 %. The Carbon-based Perovskite Solar Cell (C-PSC) made of a triple mesoscopic stack, namely titania, zirconia and carbon is among the most stable PSCs architectures. However, the comparison of long-term stability analysis between different laboratories is still lacking in the literature. In this work, we present the results of an Inter-Laboratory study carried out between xxx laboratories from xxx countries. The C-PSCs were prepared by the screen printing method, encapsulated, and sent to different laboratories across Europe to assess their stability applying three ISOS aging protocols: (a) in the dark (ISOS-D), (b) under simulated sunlight (ISOS-L) and (c) outdoors (ISOS-O). Over 1000 h stability is reported for devices analysed in the dark, both at room temperature and at 65 °C. Under continuous simulated sunlight of 1 sun and at open circuit, solar cells survived only for a few hours, although they recovered after being stored in the dark. An improvement in the stability is observed for cells kept at maximum power point under illumination, resembling operation in real world conditions. Finally, outdoor tests in two different locations (XXX and XXX) show that cells can operate for 30 days, with minor signs of degradation. Our findings demonstrate that open circuit conditions are too severe for stability assessment and that the diurnal variation of the PV parameters reveals performance to be strongly limited by the fill factor in the central hours of the day, due to the high series resistance of the carbon electrode. Our results unravel the most important factors affecting C-PSC lifetime which is a step forward the future commercialization of PSCs.

1. Introduction

In the wide range of possible device architectures and material combinations demonstrated so far for perovskite solar cells (PSC)[1,2], carbon-based HTM-free PSCs (C-PSC)[3] are one of the most promising, in terms of ease of manufacture and long-term stability[4] as well as environmental impact, which can be estimated via life cycle assessment (LCA)[5].

Large C-PSC modules have already been reported by different groups, with power conversion efficiency (PCE) ranging between 6 and 11%[4,6–10], and efforts have been focused so far on improving the manufacturing process: introducing NIR sintering to reduce the processing time to just tens of seconds[10], and a robotic mesh infiltration technique for a fast and homogeneous deposition of the perovskite, even on large areas[11]; optimising the printing process through accurate registration of layers[4,6,8,9]; demonstrating laser patterning and mechanical scribing as effective methods to increase modules' geometrical fill factor (ratio of active area over the total area).

When considering small cells (≤ 1 cm^2 of active area), C-PSCs lag behind other PSC architectures that have recently exceeded 25% efficiency[12]. Regardless, a certified PCE as high as 12.84% has been reported for the $TiO_2/ZrO_2/C$ stack[3] while the record PCE ranges between 16% for a triple cation perovskite absorber, infiltrated in the same triple mesoscopic structure[13], and 17% for a PIN structure, also endowed with a triple cation perovskite plus a nickel oxide layer between the insulator and the carbon electrode[14]. Whilst lower in efficiency, C-PSC devices have, in addition to the advantages lusted earlier, demonstrated remarkable stability under illumination, both indoor at 1 sun, AM1.5 (> 1 year [4]) and outdoor (1 month, in Wuhan, China[8]; 2136 hours, i.e. 89 days, location: 39°19′48″N 114°37′26″E, China[16]). Combined with the advantages listed

An important milestone in their development was the addition of 5-AVAI (5-ammonium valeric acid iodide) to the perovskite precursors' solution has been proved to induce the formation of a peculiar multi-dimensional 2D/3D perovskite junction, featuring both the enhanced stability of 2D perovskites and the broad absorption and excellent charge transport of 3D MAPI[4]. The AVA additive located at grain boundaries also passivate surface defects, limiting the oxygen induced degradation[15].

This work assesses the stability of such promising devices under different conditions and involves inter-laboratory studies conducted at different sites across Europe (UK, Italy, Spain, Malta) for measurements and characterisation, following the example set by the OPV community, who has promoted and widely participated to round robins and inter-laboratory studies[17–22]. C-PSCs were manufactured by screen printing and infiltrated with AVA-MAPI solution at a single manufacturing site, encapsulated and then sent for characterisation at different laboratories, which were tested in accordance with the ISOS protocols. Additional measurements were also performed to better understand the behaviour of such promising devices and are herein reported.

Although a long, participated and fruitful discussion about the application of the ISOS protocols to perovskite solar cells has very recently led to a consensus over procedures for assessing the stability and reporting data[23], in this work (carried out before the publication of the new consensus) the previous ISOS guidelines, agreed on by the OPV community[24], were adopted.

2. Experimental

2.1. Cells fabrication

FTO glass substrates (TEC7, XOP) were etched using a Rofin Nd:YVO4 laser (532 nm) at a speed of 150 mm s^{-1}, cleaned with Hellmanex solution in deionised water, washed with deionised water and rinsed in acetone and isopropanol, before being O_2 plasma treated. A 50 nm-thick compact TiO_2 layer was deposited via spray pyrolysis at 300°C from a solution 1:9 of titanium di-isopropoxide bis(acetylacetonate) (Sigma) in isopropanol. The triple mesoporous stack was obtained via screen printing of commercial pastes: first, the TiO_2 layer (30 NRD Dyesol, diluted 1:1 by weight with terpineol), followed by sintering at 550°C for 30 minutes; then the ZrO_2 layer (Solaronix), sintered at 400°C for 30 minutes; finally, the carbon layer (Gwent Electronic Materials), sintered at 400°C for 30 minutes. A solution of AVAI, MAI and PbI_2 in GBL was prepared according to Jiang et al [25], infiltrated from the top carbon electrode and annealed in a fan oven at 50°C for 1 hour. Silver paint was applied to the contacts and cells were encapsulated in air using a glass cover on top of the active area and a UV-curable epoxy around the edges (Figure 1). The active area was masked to 0.5 cm^2 by using laser-cut black adhesive masks. Cells destined to outdoor testing had wires soldered onto the contacts (Figure 1), an additional waterproof silicone edge sealing, applied before starting the test, and a UV filter. All cells were masked before being shipped to ensure the same active area to be measured in different labs.

2.2. ISOS tests

Prior to shipping, the cells were characterised at the manufacturer laboratory, performing JV and EQE measurements. Once received by the characterization laboratory and before starting the stability tests, they were measured again, using the same settings as in the manufacturing laboratory: 20 mV/s, for both reverse and forward scans between 1 V and -0.1 V.

Indoor tests (both dark and light, D1 D2 L1 L2):

Outdoor tests in Barcelona, Spain (ISOS O2), April-May 2017: Encapsulated cells with UV filter and masks. 2-axys tracking system, forward and reverse J-V curves every ~45 min when irradiance > 50 W/m^2 (sweep rate 20 mV/s)

An irradiance threshold of 50 W/m^2 (measured by the pyranometer on the solar tracker) was set as the criteria for performing the IV measurement.

Outdoor tests in Paola, Malta (O2? Were cells measured in situ?),:

2.3. *Further characterisation*

The morphology of the mesoporous stack was studied using a JEOL-JSM-7800F field emission scanning electron microscope (5 kV acceleration voltage, a working distance of 10 mm and a magnification of x25,000).

Steady state and transient measurements:

Raman measurements were performed with a Renishaw Invia Raman system in backscattering configuration. A 532 nm laser and 50x objective were used (NA: 0.50, spot size ≈ 1 μm). A laser power of 0.3 mW and acquisition time of 5 s were used. For each sample, 100 different spots were measured over the surface and averaged to increase the signal-to-noise ratio without degrading the cell by long laser exposure. The samples were analysed from both the carbon side and glass side to probe the perovskite degradation in the carbon or mesoporous TiO_2 film, respectively.

3. Results and discussion

Figure 1 shows the cross-sectional view of the typical C-PSC used for this study: on an FTO-glass covered by a very thin compact TiO_2 (c-TiO_2), deposited by spray pyrolysis, three printed mesoporous layers overlapped: titania (m-TiO_2), zirconia (m-ZrO_2) and carbon. While the former two layers have similar porosity and account for around 2 μm of the device final thickness (being TiO_2 nearly 800 nm and ZrO_2 1.2 μm), the carbon layer is over 10 μm thick and made of both large graphite flakes and fine carbon black particles, as shown by the cross-section SEM. The AVA-MAPI precursors solution was infiltrated from the top through the carbon and percolated throughout the mesoporous stack down to the TiO_2, filling the pores and, within them, slowly crystallizing into perovskite during the annealing at 50 °C.

Prior to testing, silver paint was applied to the contacts and a black tape mask to the glass side, with an aperture of 0.5 cm^2 to univocally define the active area, allowing consistency for samples measured in different laboratories.

All cells were encapsulated in air using a plain glass cover and a UV-curable epoxy for edge sealing (primary encapsulation). Curing was performed under a UV lamp for few seconds, having care of exposing only the epoxy around the glass cover edges. Cells meant for outdoor testing had wires ultrasonically soldered to the contacts to make possible the addition of a UV filter and a secondary encapsulation (Figure S1).

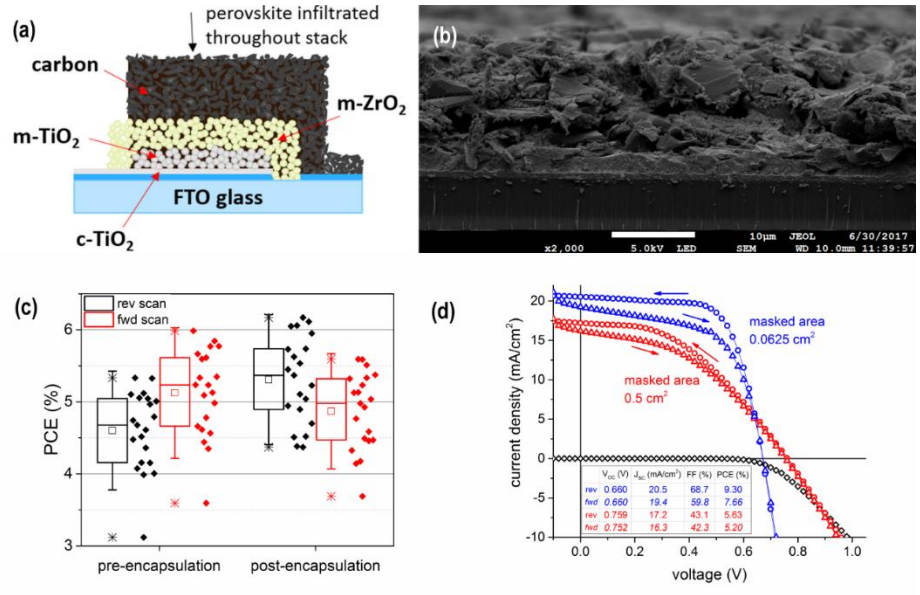

Figure 1. (a) schematics and (b) cross-section SEM image of a C-PSC, showing the different layers forming the device; (c) PCE distribution before and after encapsulation for 21 cells, masked to 0.5 cm^2 area; (d) typical JV curves for a cell with different masked areas. Scans were performed from 1 V to -0.1 V at 20 mV/s, in both reverse (V_{OC} to J_{SC}) and forward directions.

Photovoltaic performance of As-prepared devices. J-V measurements prior and after encapsulation (Figure 2a) returned a spread distribution of PCE, respectively around 4.6% and 5.4% in average for the reverse scan, but no remarkable degradation. A slight improvement in performance was noted, primarily form changes in open circuit voltage (V_{OC}) and fill factor (FF), was noted after encapsulation (Figure S2).

PCE values below 10% can be explained by the choice of carrying out all measurements on 0.5 cm^2 masked active areas: as shown in Figure 2b, reducing the masked active area to 0.0625 cm^2 boosted the PCE from 5.63% (5.20% forward scan, 5.4% stabilized at maximum power point – Figure S3) up to 9.30% (7.66% forward scan). As reported for similar cells infiltrated with MAPI[10], the dependence of the performance on the masked area is due to limitations in the conductivity of the carbon layer, affecting the series resistance, thus the fill factor (FF), as clearly shown by the slope of the J-V curve around V_{OC}. J_{SC} values also depended on the masked area, denoting a non-homogenously infiltrated perovskite, possibly hindered by dense carbon flakes[26]. Despite the lower performance, 0.5 cm^2 masks were used throughout the study to allow sampling a more representative portion of the devices. IPCE spectra returned values of integrated J_{SC} consistent with those obtained by the J-V scans under the solar simulator (Figure S3). Devices were shipped by air to the other partners for stability assessment and further characterisation, as detailed in Table 1.

Table 1. Number of cells shipped to the different partners and tests performed, according to the ISOS definition.

No. of cells	*Tests*	*Laboratory*
12	ISOS D1, D2, L1, L2	Bangor University (Wales)
2	ISOS O2	ICN2 Barcelona (Spain)
2	ISOS O2	MCAST Paola (Malta)
2	Raman spectroscopy	Swansea University (UK)
2	Steady state and transient measurements	University of Rome Tor Vergata (Italy)

Encapsulated cells underwent different stability tests, following the ISOS testing protocols, both in the dark and under continuous light illumination. In the dark, both at room temperature (ISOS D1) and at 65 °C (ISOS D2), the devices proved to be remarkably stable. Interestingly, at room temperature (Figure 3, top), they suffered from an initial loss in performance, primarily due to a decrease of the V_{OC} (Figure S 3), which led to a drop of around 20% in the initial PCE in 75 hours (T_{80}), although this stabilised afterwards without any further decrease for over 1000 hours. By contrsast, when subjected to elevated temperature at 65 °C (Figure 3, bottom), the cells experienced a 20% improvement in the average performance within the first 3-4 hours, which was maintained for almost 2000 hours, without seeing any further drop in performance. In this case though, the V_{OC} decreased in the first few hours but this was offset by an increase in the J_{SC} (Figure S 4), leading to the overall PCE improvement. It is likely that the exposure to elevated temperatures led to further annealing of the absorber layer with an improvement of the perovskite crystallinity and/or interfaces quality, i.e. better contact between perovskite and mesoscopic layers.

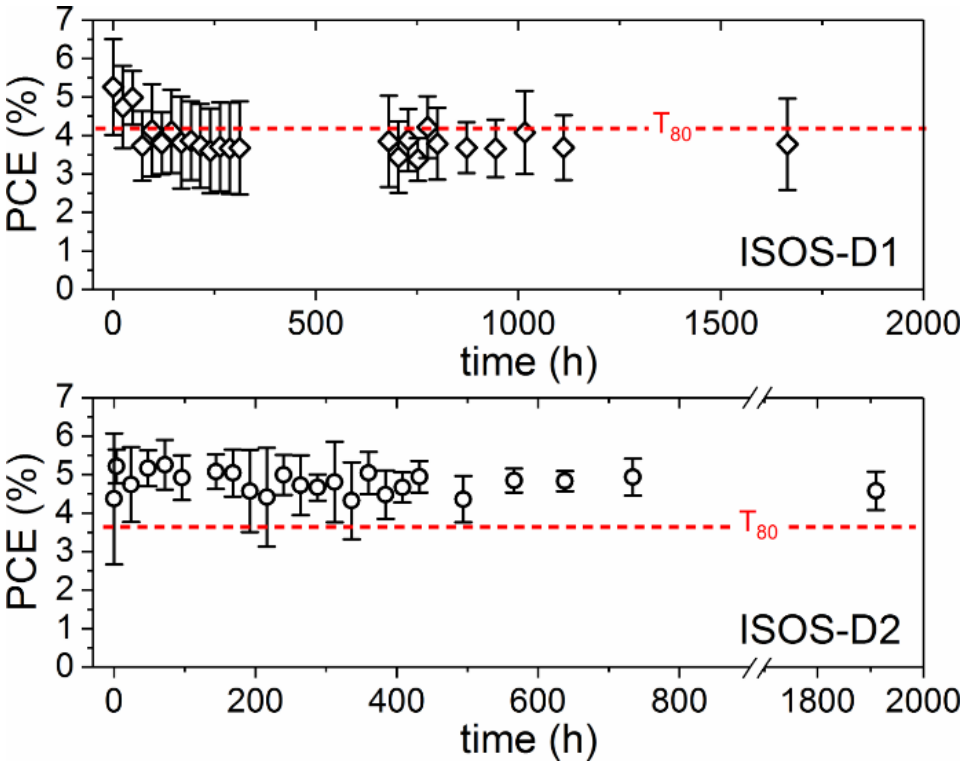

Figure 2. ***ISOS-D1*** *(dark, room temperature, ambient humidity) and* ***ISOS-D2*** *stability tests (dark, 65 °C, ambient humidity): performance over time (average of 3 cells, 0.5 cm² masked area). The dashed line indicates T_{80} value, i.e. the time when the PCE drops to 80% of its initial value. The remaining PV parameters are reported in Figure S 3 and Figure S 4.*

With respect to the devices aged in the dark, Raman spectroscopy was adopted to probe the degradation products within a perovskite device stack. One of the main by-products of perovskite degradation is lead iodide (PbI_2), which has a strong Raman signal, when excited with 532 nm laser[27], and such signal intensity is sensitive to the amount of PbI_2 formed in the perovskite, which can then be related to the film and/or device degradation. Such a signal can be detected as long as sufficient light reaches the PbI_2 formed at the interfaces and/or in the bulk of the perovskite film.

In a carbon-based PSC, the perovskite is infiltrated all the way through the mesoporous layers. Hence, the perovskite and degradation products formed within the perovskite can be detected and monitored either from the glass/m-TiO_2 side or from the air/carbon side. $CH_3NH_3PbI_3$ has a penetration depth of approximately 500 nm at 532 nm excitation wavelength, which is much less than the total thickness of the carbon layer (i.e. >10 μm). Thus, the Raman signal from the carbon side will be indicative of perovskite and PbI_2 formed near the surface of the carbon layer only. On the other hand, measuring the device stack from the glass side will give information about perovskite and degradation products formed in the mesoporous TiO_2 layer only (~ 700 nm thick), i.e. in the photoactive part of the stack, where charge carriers are generated.

Raman measurements were thus performed on encapsulated cells, before and after ageing for 1200 h in the dark at room temperature and ambient humidity (ISOS-D1), and on non-encapsulated devices for comparison.

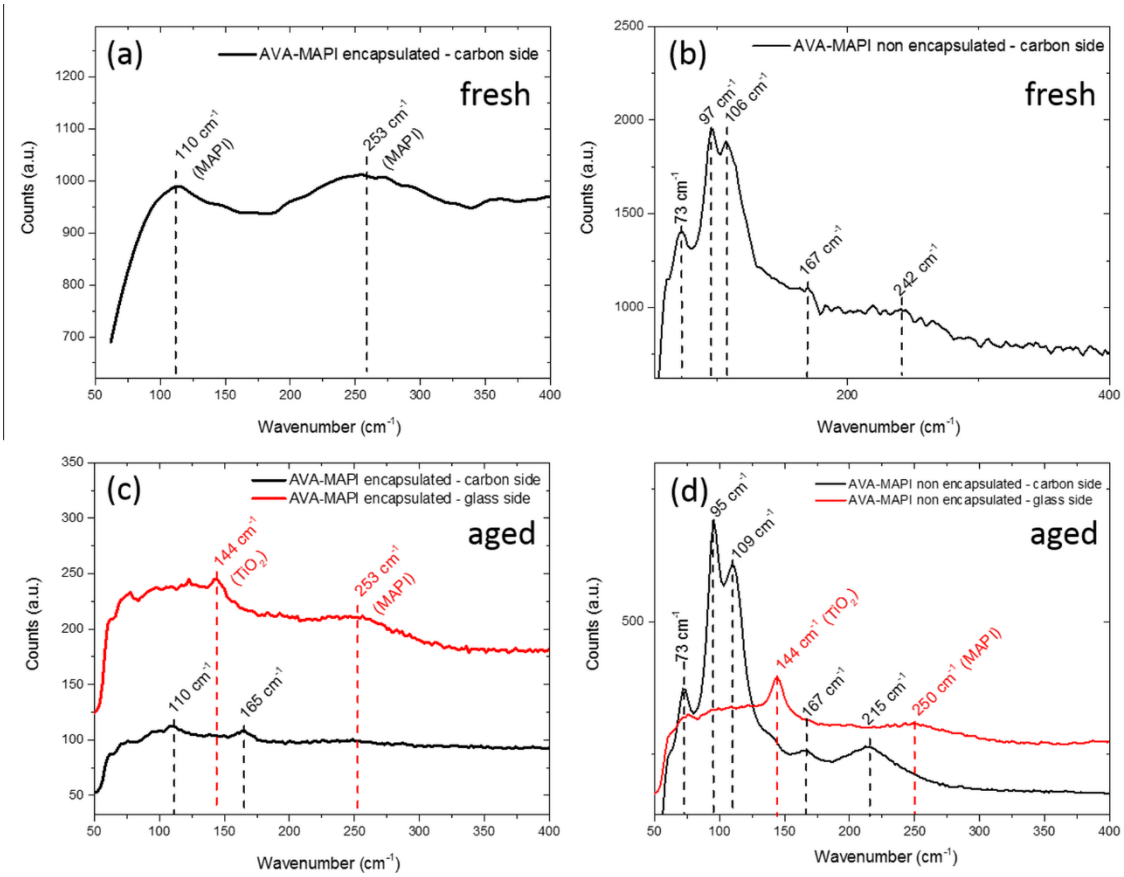

Figure 3. ***Raman spectra:*** *freshly prepared, encapsulated (a) and not encapsulated (b) cells; aged for 1200 h in the dark at room temperature and ambient humidity (ISOS-D1), encapsulated (c) and not encapsulated (d). Black spectra were measured from the carbon side whilst red spectra from the glass/titania side.*

The Raman spectra for the fresh encapsulated and non-encapsulated samples measured from the carbon side are shown in Figure 3a and b. For the encapsulated sample, typical Raman spectrum of $CH_3NH_3PbI_3$ is observed with two broad and weak peaks at 110 cm^{-1} and 250 cm^{-1}, which were assigned to the librational and torsional modes of the methyl ammonium (MA) cations, respectively [Quarty]. For the non-encapsulated sample, a completely different spectrum is measured which shows sharp and intense peaks at 73 cm^{-1}, 96 cm^{-1} and 106 cm^{-1} indicatives of the presence of a large amount of PbI_2 near the carbon surface, along with non-degraded perovskite, as revealed by the broad and poorly resolved peak between 200 cm^{-1} and 300 cm^{-1}. Hence, the perovskite film near the surface of the device has already initiated degradation shortly after fabrication due to exposure to air when the device is not encapsulated, since some PbI_2 is formed alongside $CH_3NH_3PbI_3$.

After aging, different spectra are observed when measuring the devices from the carbon side (Fig. 3c and d, black lines). In the case of the encapsulated sample, no PbI_2 is measured near the surface but two small peaks at 110 cm^{-1} and 165 cm^{-1} were observed, which could be due to the formation of dihydrate perovskite $(CH_3NH_3)_4PbI_6{\cdot}2H_2O$, as shown in an earlier report[27]. Thus, the encapsulating glass seems to work as a barrier to environmental moisture and oxygen, preventing the degradation of the perovskite to PbI_2. However, the presence of dihydrate perovskite indicates that small amount of water could have been trapped in the stack during the fabrication process and/or the encapsulation, both carried out in air. For the non-encapsulated sample, intense PbI_2 signal is measured from the carbon side, and the perovskite Raman bands are not observed anymore (the peak at 215 cm^{-1} is also

due to PbI_2). This clearly indicates the conversion of perovskite to PbI_2 in the carbon layer, near the surface, during the aging process.

By contrast, when the aged samples are measured from the mesoporous TiO_2 side (Fig. 3c and d, red lines), no PbI_2 is detected for neither the encapsulated nor the non-encapsulated samples. Instead, a broad band at 250 cm^{-1} indicates non-degraded perovskite and the peak at 144 cm^{-1} matches with anatase TiO_2 [Tian JPCC 2012]: the perovskite infiltrated within the mesoporous TiO_2 layer was well preserved and did not undergo any major degradation, even without encapsulation. This correlates well with the performance of the devices, as summarized in Table S 1: there is no degradation of the efficiency after 1200 h aging for both the encapsulated and non-encapsulated samples, and even a slight improvement in reverse bias. Indeed, Raman measurements showed that although the perovskite is degraded in the carbon electrode without encapsulation, it remains unchanged in the photoactive layer where charges are generated (Figure S6), which explains the good stability in the dark of both the encapsulated and non-encapsulated carbon-based PSC.

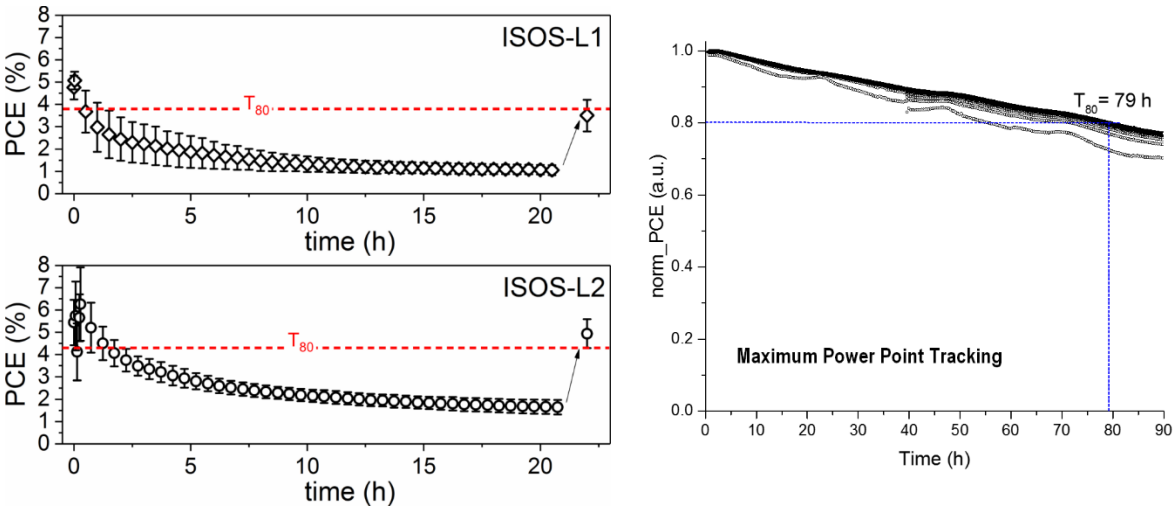

Figure 4. Light soaking tests on encapsulated cells: (top left) ***ISOS-L1*** *at room temperature and ambient humidity (bottom left) and* ***ISOS-L2*** *at 65 °C and ambient humidity. Reported data are averaged values over 3 devices with 0.5 cm^2 masked area. The cells were tested again once shipped back to the manufacturing laboratory, showing partial recovery. (right) Light soaking under LEDs at 1 equivalent sun, P&O MPP tracking.*

The high stability observed under ISOS-D1 and D2 conditions was not replicated under continuous illumination at open circuit at room temperature (in accordance with ISOS-L1 tests) nor at 65°C (ISOS-L2): in both instances, the performance dramatically dropped in few hours, regardless the temperature (Figure 4). It is well known that an open circuit bias can accelerate the degradation during light soaking tests[23]: non extracted photogenerated charges accumulate and lead to high concentrations of radicals, which, in presence of oxygen and light, degrade the device[15,28].

Several reports have demonstrated PSCs can recover in performance after leaving the devices in the dark for a controlled amount of time[23,29]. Cells used for ISOS-L1 and L2 tests were retested X days after light soaking and they did still work, confirming that, also for this cell architecture, storage in the dark for a sufficiently long time can induce complete recovery. In this case, the recovery was only

partial, but still around the 80% of the initial value was regained, due to the combination of an irreversible J_{SC} drop of almost 50% and a slight V_{OC} rise that boosted the FF to higher values that at the beginning of the test, mitigating the loss in performance (Figure S7).

An additional light soaking test was performed under white LEDs keeping the cell at its maximum power point by P&O tracking: degradation occurred also in this case, but, as expected, at a slower rate than at open circuit, with T_{80} reached after 79 hours (Figure 4, right).

Before and after the light soaking at MPP, additional steady state tests were carried out.

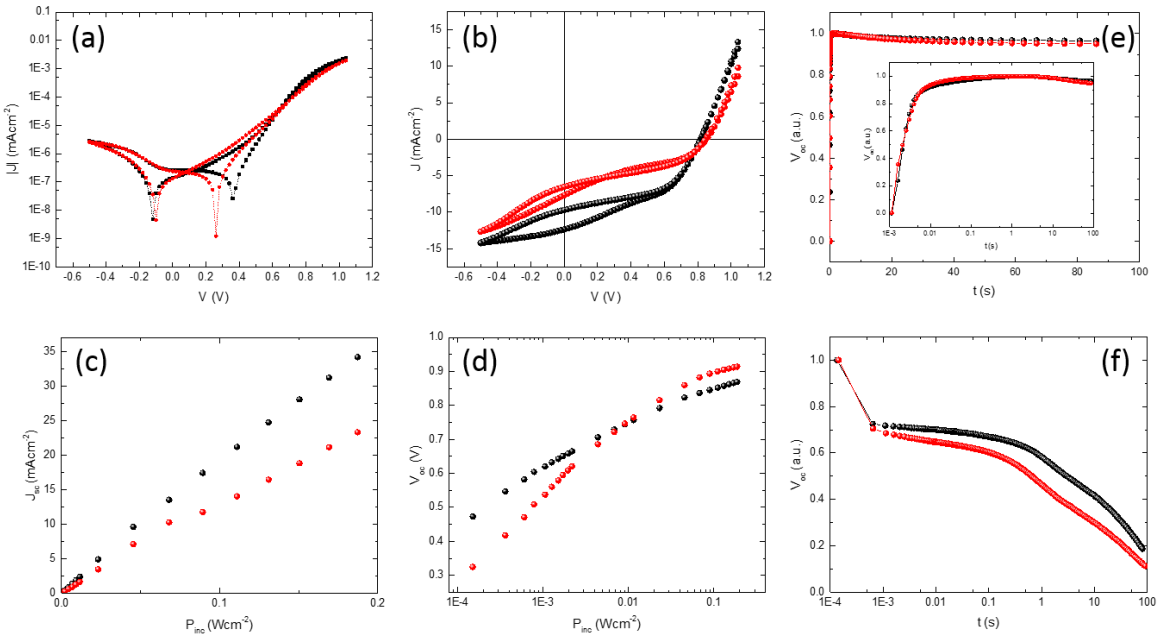

Figure 5. Comparison of C-PSCs behaviour before (black) and after (red) the light soaking under white LED at MPP (ISOS-L1): (a) dark currents; (b) reverse and forward J-V scans; (c) Jsc and (d) Voc at different light intensities; (e) Voc rise; (f) Voc decay.

Finally, outdoor measurements were carried out accordingly to the ISOS-O2 protocol in two different sites, i.e. Barcelona, Spain (41.30°N, 2.09°W) and Paola, Malta (**add coordinates**). In both locations, as shown in Figure 6, cells were stable for several weeks (between 700 and 800 hours, i.e. around 30 days), adding further evidence of the good outdoor performance of this PSC architecture to the already published reports of one-week stability in Jeddah, Saudi Arabia[30], 30 days in Wuhan, China[8] and nearly 90 days in location 39°19'48"N 114°37'26"E, China, with temperatures ranging between -10 and 35 °C[16].

As the tests were carried out between April and June (late spring – summer at the given latitudes) in Southern Europe, temperatures were above 20 °C during the central hours of the day and above 6 °C at night, whereas irradiation levels of about 1000 W/m^2 were achieved around midday in sunny days. Irradiance levels dropped during cloudy days and so did the photogenerated current, but overall the

performance was not affected, as the detrimental effect on J_{SC} was offset by the FF improvement. Cells were checked after being removed from the tracking system by measuring their IPCE: little variation is observed compared to the spectrum at the beginning of the test (Figure S 10).

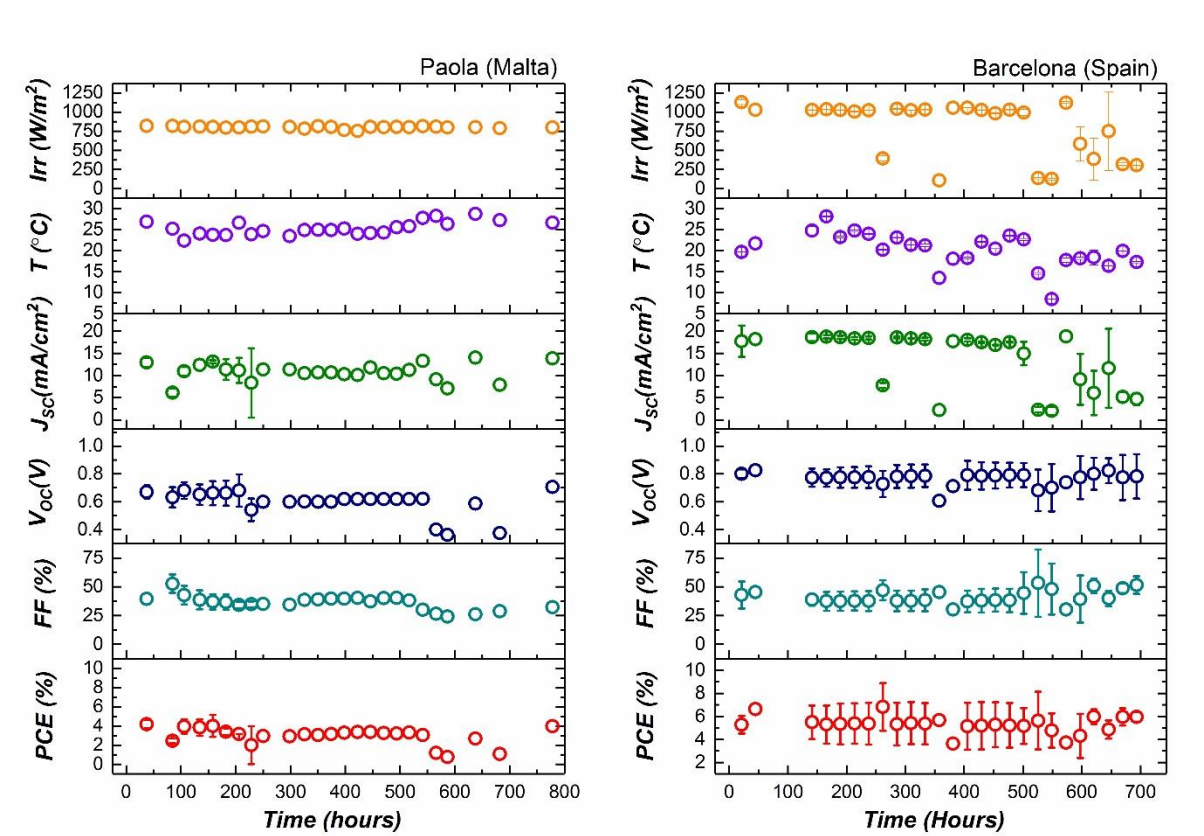

*Figure 6. Stability analysis carried out to C-PSCs under protocol **ISOS-O2** (outdoor tests): irradiance, temperature and PV parameters over time for encapsulated cells tested in Paola, Malta (left, May-June) and Barcelona, Spain (right, April-May). In each location, 2 devices were tested (in Paola, one cell stopped working after 250 hours). Plotted data refer to midday measurements.*

Although Figure 6 shows only midday values of the recorded temperature, irradiance and PV parameters, in one site (Barcelona), C-PSC outdoor operation was also tracked from early morning to late evening, making possible single-day analysis of the device response under variable irradiation levels and temperatures. J-V curves were performed every 45 minutes, at a scan rate of 20 mV/s in both forward and reverse direction. The evolution of all the parameters over 3 days, from around 8:00 am to around 8:00 pm, is shown in Figure 7. Temperatures were lower in the morning, high and quite constant in the central hours and still around 20 °C even in the late evening. The J_{SC} trend mimicked the evolution of the irradiation and V_{OC} was fairly constant over the hours, with a slight drop at about 8 am and 8 pm. Large FF values were observed in the early morning and late evening while they significantly dropped in the central hours when the temperature and irradiation were around their maximum: the high series resistance of the carbon electrode affected the FF as the irradiation levels and the photogenerated currents increased, limiting the PCE in the central hours of the day. Temperature as well as variable spectral composition of sunlight during the day could explain the asymmetrical PCE trend, with the highest values in the late evening. It is worth noting that a similar behaviour (higher PCE values at the beginning and end of the day) has been reported also for NiOx/MAPI/PCBM[31] and m-TiO_2/mixed cation-halide perovskite/spiro[32] devices.

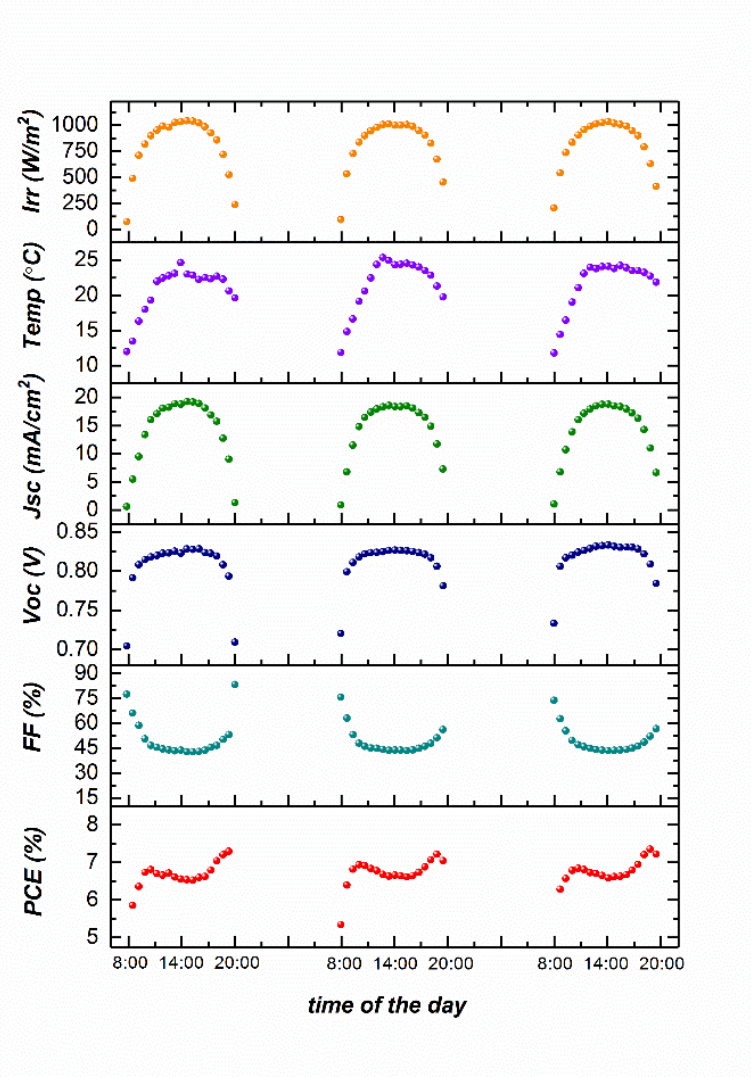

*Figure 7. Stability analysis carried out for C-PSCs under protocol **ISOS-O2** (outdoor tests): evolution of irradiance, temperature and PV parameters during daytime over 3 consecutive days for an encapsulated solar cell analysed in Barcelona, Spain.*

As for other PSC architectures, the response of these C-PSC devices in terms of stability depend on the applied ageing conditions and can be explained by the different types of degradation, i.e. reversible or permanent, that are triggered in each case. As already reported for mixed cation-halide perovskites on both m-TiO_2 and SnO_2 based cells[29,32,33], this work demonstrated that also printable C-PSC cells can degrade beyond the threshold of reversible losses under continuous illumination (faster at open circuit than when tracking the maximum power point) and have their efficiency dropping quickly, even if a partial recovery is possible upon a long enough time of storage in the dark; whereas, over light/dark cycles such as in an outdoor test, the degradation can be reversible and cells recover overnight, leading to a remarkable ~30 days stable operation in two different sites.

4. Conclusions

We have carried out an Inter-Laboratory stability analyses of C-PSCs fabricated under controlled conditions by different laboratories. Analyses were carried out following several ISOS protocols (ISOS-

D1, D2, L1, L2, O2) at different laboratories and geographical locations to assess the stability of printed, HTM-free Carob-based PSC cells based on a triple mesoscopic stack with a carbon back electrode. Whilst showing over 1000 h stability in the dark at both room temperature and 65 °C, these devices suffered notable performance drop when tested under continuous illumination in open circuit conditions. Maximum power point tracking and LED illumination resulted in slower degradation, as already demonstrated for other PSC architecture. Finally, cells diurnal operation was tracked for several days, showing higher PCE values in the early morning and late evening and a drop in the central hours of the day, due to the high series resistance of the carbon electrode limiting the fill factor. Nonetheless, devices were stable for about 30 days in two different sites, confirming that, also for this architecture, the natural day/night cycling, i.e. real-world conditions, is beneficial to the long-term operation and can be a more reliable way of assessing the stability.

Acknowledgements (add yours as needed)

This work was supported by the European Commission's StableNextSol COST Action MP1307.

F.D.R., Z.W. J.B., W.C.T. and T.W. would like to acknowledge the support provided from the Engineering and Physical Sciences Research Council (EPSRC) through the Self-assembling Perovskite Absorbers - Cells Engineered into Modules project (EP/M015254/1), the PhotoVoltaic Technology based on Earth-Abundant Materials project (EP/L017792/1), the High resolution mapping of performance and degradation mechanisms in printable photovoltaic devices project (EP/M025020/1) and the SPECIFIC Innovation and Knowledge Centre (EP/N020863/1); they would also like to express their gratitude to the Welsh Government for their support of the Sêr Solar programme. E.A.K. acknowledge the visiting professor fellowship from University Rome Tor Vergata.

D.T., M.L.C. and H.X. acknowledges the support from Spanish MINECO for the grant GraPErOs (ENE2016-79282-C5-2-R), the OrgEnergy Excellence Network CTQ2016-81911- REDT, the Agència de Gestiód'Ajuts Universitaris i de Recerca (AGAUR) for the support to the consolidated Catalonia research group 2017 SGR 329. ICN2 is supported by the Severo Ochoa program from Spanish MINECO (Grant no. SEV-2017-0706) and is funded by the CERCA Programme/Generalitat de Catalunya.

References

[1] S. He, L. Qiu, L. K. Ono, Y. Qi, *Mater. Sci. Eng. R Reports* **2020**, *140*, DOI 10.1016/j.mser.2020.100545.

[2] A. K. Jena, A. Kulkarni, T. Miyasaka, *Chem. Rev.* **2019**, *119*, 3036–3103.

[3] A. Mei, X. Li, L. Liu, Z. Ku, T. Liu, Y. Rong, M. Xu, M. Hu, J. Chen, Y. Yang, et al., *Science (80-.).* **2014**, *345*, 295–298.

[4] G. Grancini, C. Roldán-Carmona, I. Zimmermann, E. Mosconi, X. Lee, D. Martineau, S. Narbey, F. Oswald, F. De Angelis, M. Graetzel, et al., *Nat. Commun.* **2017**, *8*, 1–8.

[5] J.-A. Alberola-Borràs, J. A. Baker, F. De Rossi, R. Vidal, D. Beynon, K. E. A. Hooper, T. M. Watson, I. Mora-Seró, *iScience* **2018**, (accepted).

[6] A. Priyadarshi, L. J. Haur, P. Murray, D. Fu, S. Kulkarni, G. Xing, T. C. Sum, N. Mathews, S. G. Mhaisalkar, *Energy Environ. Sci.* **2016**, *9*, 3687–3692.

[7] A. Bashir, S. S. Shukla, J. H. Lew, S. S. Shukla, A. Bruno, D. Gupta, T. Baikie, R. Patidar, Z. Akhter, A. Priyadarshi, et al., *Nanoscale* **2018**, *10*, 2341–2350.

[8] Y. Hu, S. Si, A. Mei, Y. Rong, H. Liu, X. Li, H. Han, *Sol. RRL* **2017**, *1*, 1600019.

[9] F. De Rossi, J. A. Baker, D. Beynon, K. E. A. Hooper, S. M. P. Meroni, D. Williams, Z. Wei, A. Yasin, C. Charbonneau, E. H. Jewell, et al., *Adv. Mater. Technol.* **2018**, 1800156.

[10] J. Baker, K. Hooper, S. Meroni, A. Pockett, J. McGettrick, Z. Wei, R. Escalante, G. Oskam, M. Carnie, T. Watson, *J. Mater. Chem. A* **2017**, *5*, 18643–18650.

[11] S. M. P. Meroni, Y. Mouhamad, F. De Rossi, A. Pockett, J. Baker, R. Escalante, J. Searle, M. J. Carnie, E. Jewell, G. Oskam, et al., *Sci. Technol. Adv. Mater.* **2018**, *19*, 1–9.

[12] NREL, "Best Research-Cell Efficiency Chart | Photovoltaic Research | NREL," **2019**.

[13] Q. Wang, W. Zhang, Z. Zhang, S. Liu, J. Wu, Y. Guan, A. Mei, Y. Rong, Y. Hu, H. Han, *Adv. Energy Mater.* **2019**, 1903092.

[14] S. Liu, W. Huang, P. Liao, N. Pootrakulchote, H. Li, J. Lu, J. Li, F. Huang, X. Shai, X. Zhao, et al., *J. Mater. Chem. A* **2017**, *5*, 22952–22958.

[15] C. T. Lin, F. De Rossi, J. Kim, J. Baker, J. Ngiam, B. Xu, S. Pont, N. Aristidou, S. A. Haque, T. Watson, et al., *J. Mater. Chem. A* **2019**, *7*, 3006–3011.

[16] Z. Fu, M. Xu, Y. Sheng, Z. Yan, J. Meng, C. Tong, D. Li, Z. Wan, Y. Ming, A. Mei, et al., *Adv. Funct. Mater.* **2019**, *29*, 1809129.

[17] F. C. Krebs, S. A. Gevorgyan, B. Gholamkhass, S. Holdcroft, C. Schlenker, M. E. Thompson, B. C. Thompson, D. Olson, D. S. Ginley, S. E. Shaheen, et al., *Sol. Energy Mater. Sol. Cells* **2009**, *93*, 1968–1977.

[18] S. A. Gevorgyan, A. J. Medford, E. Bundgaard, S. B. Sapkota, H. F. Schleiermacher, B. Zimmermann, U. Würfel, A. Chafiq, M. Lira-Cantu, T. Swonke, et al., *Sol. Energy Mater. Sol. Cells* **2011**, *95*, 1398–1416.

[19] S. A. Gevorgyan, M. V Madsen, H. F. Dam, M. Jørgensen, C. J. Fell, K. F. Anderson, B. C. Duck, A. Mescheloff, E. A. Katz, A. Elschner, et al., *Sol. Energy Mater. Sol. Cells* **2013**, *116*, 187–196.

[20] S. A. Gevorgyan, M. Corazza, M. V Madsen, G. Bardizza, A. Pozza, H. Müllejans, J. C. Blakesley, G. F. A. Dibb, F. A. Castro, J. F. Trigo, et al., *Polym. Degrad. Stab.* **2014**, *109*, 162–170.

[21] M. V Madsen, S. A. Gevorgyan, R. Pacios, J. Ajuria, I. Etxebarria, J. Kettle, N. D. Bristow, M. Neophytou, S. A. Choulis, L. Stolz Roman, et al., *Sol. Energy Mater. Sol. Cells* **2014**, *130*, 281–290.

[22] T. T. Larsen-Olsen, S. A. Gevorgyan, R. R. Søndergaard, M. Hösel, Z. Gu, H. Chen, Y. Liu, P. Cheng, Y. Jing, H. Li, et al., *Sol. Energy Mater. Sol. Cells* **2013**, *117*, 382–389.

[23] K. Domanski, E. A. Alharbi, A. Hagfeldt, M. Grätzel, W. Tress, *Nat. Energy* **2018**, *3*, 61–67.

[24] M. O. Reese, S. A. Gevorgyan, M. Jørgensen, E. Bundgaard, S. R. Kurtz, D. S. Ginley, D. C. Olson, M. T. Lloyd, P. Morvillo, E. A. Katz, et al., *Sol. Energy Mater. Sol. Cells* **2011**, *95*, 1253–1267.

[25] X. Jiang, Y. Xiong, A. Mei, Y. Rong, Y. Hu, L. Hong, Y. Jin, Q. Liu, H. Han, *J. Phys. Chem. Lett.*

2016, *7*, 4142–4146.

[26] H. Lakhiani, T. Dunlop, F. De Rossi, S. Dimitrov, R. Kerremans, C. Charbonneau, T. Watson, J. Barbé, W. C. Tsoi, *Adv. Funct. Mater.* **2019**, *29*, 1900885.

[27] K. E. A. Hooper, H. K. H. Lee, M. J. Newman, S. Meroni, J. Baker, T. M. Watson, W. C. Tsoi, *Phys. Chem. Chem. Phys.* **2017**, *19*, 5246–5253.

[28] D. Bryant, N. Aristidou, S. Pont, I. Sanchez-Molina, T. Chotchunangatchaval, S. Wheeler, J. R. Durrant, S. A. Haque, *Energy Environ. Sci.* **2016**, DOI 10.1039/C6EE00409A.

[29] M. V. Khenkin, K. M. Anoop, I. Visoly-Fisher, S. Kolusheva, Y. Galagan, F. Di Giacomo, O. Vukovic, B. R. Patil, G. Sherafatipour, V. Turkovic, et al., *ACS Appl. Energy Mater.* **2018**, *1*, 799–806.

[30] X. Li, M. Tschumi, H. Han, S. S. Babkair, R. A. Alzubaydi, A. A. Ansari, S. S. Habib, M. K. Nazeeruddin, S. M. Zakeeruddin, M. Grätzel, *Energy Technol.* **2015**, *3*, 551–555.

[31] V. Stoichkov, N. Bristow, J. Troughton, F. De Rossi, T. M. Watson, J. Kettle, *Sol. Energy* **2018**, *170*, 549–556.

[32] Y. Reyna, M. Salado, S. Kazim, A. Pérez-Tomas, S. Ahmad, M. Lira-Cantu, *Nano Energy* **2016**, *30*, 570–579.

[33] K. Domanski, B. Roose, T. Matsui, M. Saliba, S. H. Turren-Cruz, J. P. Correa-Baena, C. R. Carmona, G. Richardson, J. M. Foster, F. De Angelis, et al., *Energy Environ. Sci.* **2017**, *10*, 604–613.